Reliable Dense-Gas Tracers at High Redshift: CN in the z $\sim$ 4 Quasar APM 08279

© **R. Soria-Ruiz, S. García-Burillo, A. Usero**

Observatorio Astronómico Nacional, Madrid, Spain

Molecular lines have been widely used for the study of galaxy formation and evolution at high-redshift. Of special interest is how the relation between the star formation rate and the dense-gas content varies with redshift. Fair tracers of the dense gas are key to understanding the first phases of galaxy formation. We present for the first time, the detection of the two rotational transitions CN(5–4)@115 GHz and CN(6–5)@138 GHz, in the $z \sim 4$ quasar APM 08279 with the IRAM Plateau de Bure interferometer (PdBI). Together with current information on the CN(4–3) line, we have modelled the Spectral Line Energy Distribution (SLED) of CN and derived its molecular abundance in APM 08279. Based on the previous model of the CO molecular emission from APM 08279 we have performed a preliminary analysis of the CN molecular excitation using the radiative transfer code RADEX. To reproduce the observed CN line intensities and the overall SLED, molecular abundances of $5 \cdot 10^{-8} - 5 \cdot 10^{-6}$ are needed. We conclude that the CN emission in APM 08279 is mostly free from IR pumping, and therefore is a fair tracer of the dense-molecular gas at high redshift.

Keywords: Galaxies, high-redshift, radio-lines.

1 Introduction

The lensed quasar APM 08279 is possibly the best source to study the dense gas at high redshift ($z \sim 4$). Its huge amplified IR luminosity, $\sim 10^{15} L_{\odot}$, makes it one of the most luminous objects of the universe, with a very powerful active galactic nucleus (AGN). Studies of the molecular gas in this quasar revealed the presence of a circumnuclear disk of dense and hot molecular gas, which was confirmed in multiple detections of dense gas tracers; HCN(5–4) by [6], [7], HCN(6–5) by [4], HCO^+(5–4) by [1], HCO^+(6–5) by [4], HNC(5–4) by [2] and HNC(6–5) by [4]. The detection of such highly excited molecular emission indicates that APM 08279 shows extreme physical properties of the

molecular gas which makes this galaxy a unique and extreme case for which no counterpart has been found yet.

However, the scenario explaining the high intensities of the lines of some molecular species like HCN or HCO^+ relative to CO observed in APM 08279 is still debated. Theoretical models of the HCN excitation indicate that collisional excitation cannot account alone for the observed high HCN line intensities. The mechanism proposed by [7] and [4] to boost the HCN is by IR radiation. In the context of the best possible fit to the observational data, these authors argue that the HCN emission is dominated by IR pumping, indicating that the standard conversion factors for HCN overpredict the dense molecular gas mass, and that models do not require exceptional high relative abundances of HCN. Should this scenario applies to other AGN-dominated sources, like APM 08279, the quest for a reliable tracer of the dense gas would be needed in a significant fraction of high–z galaxies.

2 Observations and results

We used the IRAM PdBI to observe the CN(5–4) and CN(6–5) rotational lines in APM 08279. The observations were performed with five antennas in D configuration in 2009. The correlator was configured to $z = 3.9118$ and centered on redshifted CN(5–4) and (6–5) frequencies (115.40 GHz and 138.47 GHz) with effective bandwidths of 1000 MHz ($\sim$ 2600 km s^{-1}) and 3600 MHz ($\sim$ 7800 km s^{-1}) respectively. The absolute flux scale was derived from amplitude calibrations on nearby quasars and was determined within 10 % accuracy. Data calibration and analysis were done following the standard procedures using the GILDAS software. All the maps shown have been shifted to a common reference, the phase tracking center of the CN(5–4) observation (RA=$08^{\rm h}31^{\rm m}41\overset{\rm s}{.}73$, Dec= $52^\circ\,45'\,17\overset{''}{.}4$).

Fig. 1 shows the spectrum of the CN(5–4) emission (continuum and spectral line) with a velocity resolution of 100 km s^{-1}. The line width is FWHM = $= 525 \pm 113$ km s^{-1} and the central velocity $(v - v_0)$ = (-60 ± 47) km s^{-1}. We estimated the continuum emission to be (1.8 ± 0.12) mJy by combining the data with velocities below -500 km s^{-1} and above 500 km s^{-1} (labelled I and III). The CN(5–4) line emission is detected in the [–500 , 500] km s^{-1} velocity range (interval II). The integrated intensity map shows a clear $\sim 6\sigma$ detection of (1.02 ± 0.16) Jy km s^{-1}. Following [5], this translates into a luminosity $L'_{\rm line}$= (2.67 $\pm$ 0.4) 10^{10} K km s^{-1} pc^2. The spectrum of the CN(6–5) emission (continuum and spectral line) with a velocity resolution of 87 km s^{-1}is shown in Fig. 2. The Gaussian fit gives a line width of (440 ± 100) km s^{-1} and a central velocity of $(v - v_0)$ = (45 ± 46) km s^{-1}. The continuum emission was estimated to be (3.7 ± 0.11) mJy, and it was determined from the wide spectrum ($\sim$ 3.6 GHz) line-free channels (velocities < -500 km s^{-1}and > 500 km s^{-1},

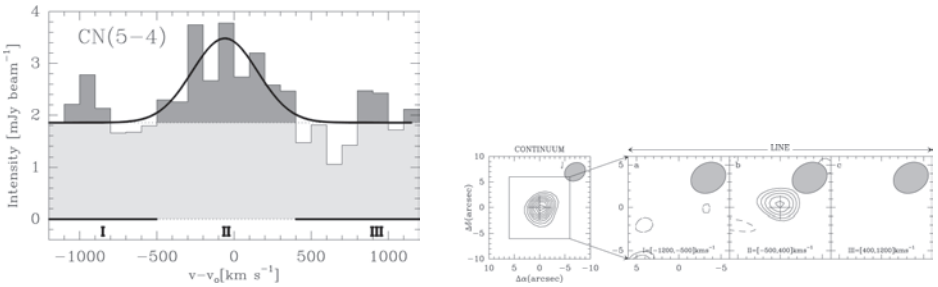

Fig. 1. *Left*: Spectrum of the CN(5–4) emission in APM 08279. *Right*: Continuum and line velocity-integrated emission maps of APM 08279. The continuum map has been derived using velocity intervals I and III and the line emission maps using velocity interval II. Contour levels are $-3\,\sigma$ and $3\,\sigma$ to $14\,\sigma$ in steps of $1.5\,\sigma$ ($1\,\sigma$ = = 0.12 mJy km s^{-1}) in the continuum map and $-3\,\sigma$ and $3\,\sigma$ to $6\,\sigma$ in steps of $1\,\sigma$ ($1\,\sigma = 0.16$ Jy km s^{-1}) for the line maps.The filled ellipses represent the $4\farcs31 \times 3\farcs48$ synthesized beam

which includes intervals I and III of Fig. 2). Continuum and line channel maps were also obtained (see Fig. 2). The CN(6–5) line emission is detected in the [–500 , 500] km s^{-1} velocity range (interval II). From the integrated intensity map we derive a $\sim 6\sigma$ detection of (0.72 ± 0.12) Jy km s^{-1}, which translates into a luminosity $L'_{\rm line}$= $(1.29 \pm 0.2)\ 10^{10}$ K km s^{-1} pc^2.

3 CN molecular excitation

We have used the radiative transfer code RADEX (van der Tak et al. 2007) to reproduce the CN SLED, i. e. the line intensities, and derive the CN molecular content in APM 08279. Only collisional excitation has been considered.

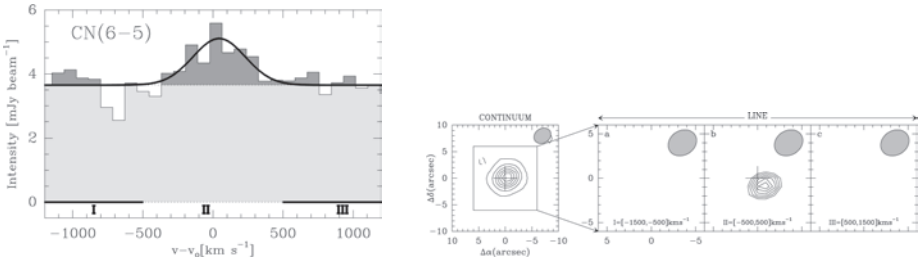

Fig. 2. *Left*: Spectrum of the CN(6–5) emission in APM 08279. *Right*: Continuum and line velocity-integrated emission maps of APM 08279. The continuum map has been derived using velocity intervals I and III and the line emission maps using velocity interval II. Contour levels are $-3\,\sigma$ and $3\,\sigma$ to $55\,\sigma$ in steps of $10\sigma (1\sigma = 0.05$ mJy km s^{-1}) in the continuum map and $-3\,\sigma$ and $3\,\sigma$ to $6\,\sigma$ in steps of $0.5\,\sigma$ ($1\,\sigma = 0.12$ Jy km s^{-1}). The filled ellipses represent the $3\farcs38 \times 2\farcs76$ synthesized beam

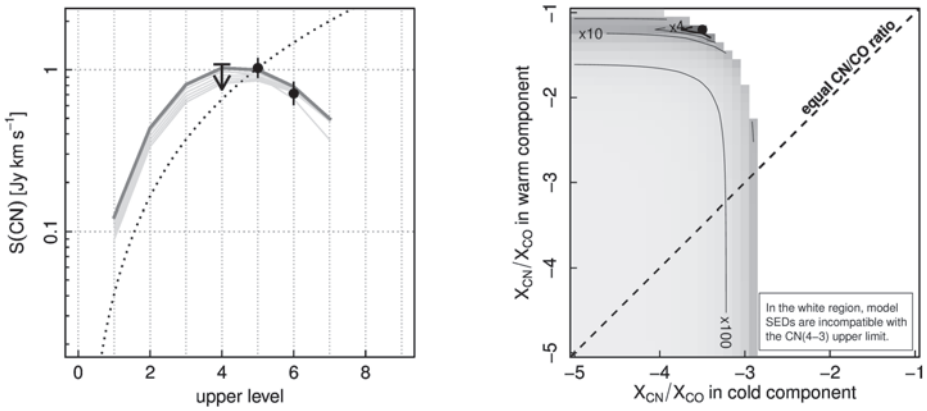

Fig. 3. Fit to the CN SLED and RADEX modelling of the CN molecular emission in APM 08279

The physical properties of the overall molecular gas, the temperature and the density, have been taken from the detailed two-phase CO model derived by [6], based on an accurate characterization of the CO SLED in APM 08279. The model has two molecular components: cold CO ($n_{\rm H_2} = 10^5$ cm^{-3} and $T_{\rm k}$ = 65 K) and warm CO ($n_{\rm H_2} = 10^4$ cm^{-3} and $T_{\rm k}$ = 220 K). Then, using the fixed values of $T_{\rm k}$ and $n_{\rm H_2}$, and a CO abundance of $8 \cdot 10^{-5}$, we have calculated the best fit for the CN SLED derived from our new line detections, together with the $3\,\sigma$ limit of CN(4–3) taken from [2], and estimated the corresponding CN abundance. Fig. 3 shows the fit to our CN data. The thick line is our best fit, while the thinner lines represent good fits with χ^2 within a factor of 4 from that of the best one. The error bars are also displayed. Also, the RADEX modelling of the CN(4–3), CN(5–4) and CN(6–5) observations is shown. The model has two free parameters: the CN/CO abundance ratios in the cold and warm phases. The plot shows the weighted sum of the squared deviations between the observations and the model (χ^2) as a function of both parameters. Darker shades correspond to lower χ^2 values, thus better fits. These are found for CN/CO abundance ratios of $6 \cdot 10^{-2}$ in the warm phase, and $6 \cdot 10^{-4}$ in the cold one. The CN abundances are then $\sim [5 \cdot 10^{-8} - 5 \cdot 10^{-6}]$, values that are compatible with current XDR models [3]. As can be seen from this preliminary theoretical approach, CN collisional excitation can account for the observed CN line intensities and reproduce the CO molecular properties. We conclude that, although CN seems to be a promising fair tracer of the dense gas, uncontaminated from IR radiation, a better characterization of the lower rotational CN lines and a further theoretical study including the IR radiation in APM 08279 are needed.

References

1. *García-Burillo S., Graciá-Carpio J., Guélin M. et al.* — 2006. — ApJ. — 645. — L17.
2. *Guélin M., Salomé P., Neri R., et al.* — 2007. — A&A. — 462. — L45.
3. *Meijerink R., Spaans M., Israel F. P.* — 2007. — A&A. — 461. — 793.
4. *Riechers D. A., Weiβ A., Walter F., et al.* — 2010. — ApJ. — 725. — 1032.
5. *Solomon P. M., Downes D., Radford S. J. E., et al.* — 1997. — ApJ. — 478. — 144.
6. *Wagg J., Wilner D. J., Neri, et al.* — 2005. — ApJ. — 634. — L13.
7. *Weiβ A., Downes D., Neri R., et al.* — 2007. — A&A. — 467. — 955.